NONLINEAR OPTICAL PHENOMENA

PACS numbers: 42.65.Ky; 42.70.Nq
DOI: 10.1070/QE2005v035n06ABEH002904

Influence of the Dember effect on second harmonic generation upon reflection of Ti : sapphire laser radiation from silicon

I.M. Baranova, K.N. Evtyukhov, A.N. Murav'ev

***Abstract*. Electronic processes stimulated in a silicon volume by a megahertz train of femtosecond pulses from a Ti : sapphire laser are studied theoretically. The spatial distribution of a photoinduced potential in the silicon volume is calculated. It is shown that this potential can considerably change a voltage applied to the near-surface region of a space charge, thereby affecting the generation of the reflected second harmonic.**

Keywords: *silicon, Ti : sapphire laser, interaction of radiation with matter, second harmonic generation, electronic processes, Dember effect.*

1. Introduction

Electronic processes stimulated by laser radiation in semiconductors and semiconductor structures play an important role in nonlinear optics of the semiconductor surface. This work is a continuation of our papers [1, 2], where the generation of the reflected second harmonic (RSH) was considered upon irradiation of silicon by a hertz train of nanosecond pulses from a Nd : YAG laser. It was shown that photostimulated electronic processes affect the nonlinear optical response, by changing the spatial charge region (SCR) near a surface. This influence is manifested, first, in the narrowing of the initial equilibrium plane near-surface SCR, caused by the presence of the surface potential $\varphi_{\rm sc}$, due to the increase in the carrier concentration. It is in this plane near-surface region that the electrostatic field is comparable to the interatomic field, which favours the RSH generation. Second, the Dember effect takes place inside a semiconductor, below the near-surface plane, thin and nonequilibrium SCR. This effect consists in the appearance of an electric field in the semiconductor volume due to the spatial inhomogeneity of the pump beam intensity and the difference in the velocities of diffusion motion of nonequilibrium electrons and holes. We will call this nonequilibrium region the Dember effect region. It was shown in [1, 2] that photostimulated electronic processes affect the RSH generation because the Dember volume potential changes the potential difference applied to the thin near-surface SCR.

The RSH generation was performed in the last years by using a Ti : sapphire laser [3, 4], whose output parameters are much better than those of a Nd : YAG laser. However, the electronic processes stimulated in semiconductors by a Ti : sapphire laser and their influence on the RSH generation have not been studied so far. We consider these questions in this paper.

2. Formulation of the problem

We used in calculations the output parameters of a Ti : sapphire laser presented in [3, 4]: the pulse duration $t_0 = 120$ fs, the pulse repetition rate $\nu = 76$ MHz, the off – duty ratio $Q = 1.10 \times 10^5$, the tuning range $\lambda = 705$ – 820 nm, and the Gaussian intensity distribution over the beam cross section $[I = I_0 \exp(-r^2/R^2)]$. For the effective beam radius $R = 0.1$ mm and the pulse energy $W = 4$ nJ, the axial intensity of the beam was $I_0 = 1.06 \times 10^{12}$ W m^{-2} and the average radiation power was $\langle P \rangle = 304$ mW. According to [3, 4], in this case the silicon surface was heated up to a few tens of degrees. Such variations in the temperature change the equilibrium concentration of carriers, but it seems that they cannot affect noticeably photostimulated processes in silicon, which are caused first of all by intense optical excitation of nonequilibrium carriers and significant gradients of the nonequilibrium concentration. However, the consideration of corrections related to thermal effects can be the subject of a separate study.

In this paper, we consider the case of radiation normally incident on the silicon surface. The optical constants of Si were taken from [5], where they were given only for discrete wavelengths, including 690.6, 731.2, 776.9, and 828.7 nm. Note that the spectral range 690.6 – 828.7 nm contains the tuning range of a Ti : sapphire laser, and absorption of radiation continuously decreases with increasing wavelength, resulting in the reduction of photostimulated electronic processes. For this reason, we estimated the maximum manifestation of these processes by using the optical constants for a wavelength of 690.6 nm, which is close to the short-wavelength boundary of the tuning range of a Ti : sapphire laser.

Table 1 presents the required parameters of silicon for the above-mentioned wavelengths: the real (n) and imaginary (κ) parts of the complex refractive index, the absorption coefficient $\alpha = 4\pi\kappa/\lambda$, the characteristic pene-

I.M. Baranova, K.N. Evtyukhov, A.N. Murav'ev Bryansk State Academy of Engineering and Technology, prosp. Stanke Dimitrov 3, 241037 Bryansk, Russia;
e-mail: ppbarano@yandex.ru, muravl@online.debryansk.ru

Received 11 October 2004; revision received 28 March 2005
Kvantovaya Elektronika **35** (6) 520 – 524 (2005)
Translated by M.N. Sapozhnikov

tration depth $d = 1/\alpha$ of radiation into silicon, the proportionality coefficient $K_g = g/I$ [g is the local photogeneration rate for electron–hole pairs and $I = I(r, z)$ is the local intensity]. For normally incident pump radiation from a medium with the real refractive index n_i (we assume that $n_i = 1$), we have $K_g = 16\pi n_i n\kappa/[(n_i + n)^2 hc]$.

Table 1. Optical parameters n, κ, α, d of silicon, the conversion coefficient K_g, the instant (g_0) and effective (g_{0e}) photogeneration rates as functions of the radiation wavelength for $t_0 = 120$ fs, $\nu = 76$ MHz, and $I_0 = 1.06 \times 10^{12}$ W m^{-2}.

Parameter	Wavelength/nm			
	690.6	731.2	776.9	828.7
n	3.796	3.752	3.714	3.673
κ	0.0130	0.0104	0.00767	0.00517
$\alpha/10^5$ m^{-1}	2.37	1.79	1.24	0.784
d/μm	4.23	5.60	8.06	12.76
$K_g/10^{23}$ J^{-1} m^{-1}	5.42	4.37	3.24	2.20
$g_0/10^{35}$ m^{-3} s^{-1}	5.75	4.63	3.43	2.33
$g_{0e}/10^{30}$ m^{-3} s^{-1}	5.24	4.22	3.13	2.12

In addition, Table 1 presents the values of the instant ($g_0 = K_g I_0$) and effective, i.e., averaged ($g_{0e} = g_0/Q$) photogeneration rates of carriers at a point where the pump intensity is maximal ($I = I_0$).

We assume that the time dependences of the local intensity $I(r, z, t)$ and photogeneration rate $g(r, z, t)$ are infinite trains of rectangular pulses beginning at the instant $t = 0$:

$$I(r, z, t) = I(r, z)f(t) = I_0 \exp\left(-\frac{r^2}{R^2} - \alpha z\right)f(t),$$
$$g(r, z, t) = g(r, z)f(t) = g_0 \exp\left(-\frac{r^2}{R^2} - \alpha z\right)f(t), \tag{1}$$

where

$$f(t) = \begin{cases} 1 & (n-1)T < t < t_0 + (n-1)T, \\ 0 & t_0 + (n-1)T < t < nT, \quad n = 1, 2, 3, \ldots; \end{cases} \tag{2}$$

T is the pulse repetition period; the coordinate z is measured inside silicon along the normal to its surface, and the radial coordinate r is measured from the beam axis.

The calculation of nonequilibrium concentrations of free electrons n' and holes p' and the electric field in the Dember effect region caused by their diffusion-drift motion is based on the solution of a set of equations including the continuity equation for electrons and holes and the Poisson equation for the Dember electric field (the surface potential in this region is screened by a plane near-surface SCR) [6]. In the cylindrical coordinate system, this set of equations has the form

$$\frac{\partial p'}{\partial t} = g(r, z, t) - \frac{1}{r}\frac{\partial}{\partial r}\left[r\left(\mu_p p' E_r - D_p \frac{\partial p'}{\partial r}\right)\right] - \frac{\partial}{\partial z}\left(\mu_p p' E_z - D_p \frac{\partial p'}{\partial z}\right) - R_p,$$

$$\frac{\partial n'}{\partial t} = g(r, z, t) + \frac{1}{r}\frac{\partial}{\partial r}\left[r\left(\mu_n n' E_r + D_n \frac{\partial n'}{\partial r}\right)\right] + \frac{\partial}{\partial z}\left(\mu_n n' E_z + D_n \frac{\partial n'}{\partial z}\right) - R_n,$$

$$\frac{1}{r}\frac{\partial}{\partial r}(rE_r) + \frac{\partial E_z}{\partial z} = \frac{e}{\varepsilon_0 \varepsilon}\left(p' - p_0 - n' + n_0\right), \tag{3}$$

$$E_r = -\frac{\partial \varphi}{\partial z}, \quad E_z = -\frac{\partial \varphi}{\partial z},$$

where μ_n, μ_p, D_n, D_p are the mobilities and diffusion coefficients of electrons and holes, respectively; R_n and R_p are the recombination terms; ε is the static dielectric constant ($\varepsilon = 11.7$ for silicon); and φ is the local potential.

As in [1, 2], we calculate the distribution of the photoinduced potential in the Dember effect region in order to determine the photoinduced change in the potential difference applied to the near-surface RSH, where one of the basic contributions to the RSH is formed. We assumed that the conditional boundary between the near-surface SCR and the region under study has the coordinate $z = 0$.

We represent the nonequilibrium concentrations of carriers in the region under study in the form

$$n' = n_0 + n_g + \eta, \quad p' = p_0 + p_g + \xi, \tag{4}$$

where n_0 and p_0 are the initial equilibrium concentrations of carriers in the electrically neutral volume of a semiconductor; n_g and p_g are the local nonequilibrium additions to the carrier concentrations caused only by two electronic processes: photogeneration and recombination; η and ξ are the nonequilibrium additions due to the diffusion-drift motion of carriers.

It is natural to assume that

$$n_g \approx p_g \gg |\eta|, |\xi|, \tag{5}$$

and, therefore, the problem can be solved in two stages. In the first stage, by neglecting diffusion-drift terms in system (3) and omitting the equation for the field, we calculate the spatiotemporal distribution of additions n_g and p_g, and in the second stage, we calculate the distributions of additions η and ξ and photoinduced electric field.

3. Calculation of nonequilibrium carrier concentrations by neglecting diffusion-drift motion

In the calculation of local additions $n_g = n_g(r, z, t)$ and $p_g = p_g(r, z, t)$ by neglecting diffusion and drift, system (3) takes the form

$$\frac{\partial n_g}{\partial t} = g(r, z)f(t) - R_n,$$
$$\frac{\partial p_g}{\partial t} = g(r, z)f(t) - R_p. \tag{6}$$

Upon intense optical excitation, the main recombination mechanisms are Auger recombination and recombination through impurity centres. Auger recombination occurs at high concentrations of nonequilibrium carriers, when $n' \approx p' \approx n_g \approx p_g \gg n_0, p_0$, and its rate is described by the expression [7]

$$R_{\rm n}^{\rm A} = R_{\rm p}^{\rm A} = a_{\rm A}(2n_{\rm g})^3 = 8a_{\rm A}n_{\rm g}^3. \quad (7)$$

For silicon, $a_{\rm A} = 4 \times 10^{-43}$ m^6 s^{-1}.

System (6) was solved numerically and analytically. In the numerical experiment, we took into account both Auger recombination and recombination through impurity centres – doubly charges gold ions. The expressions for recombination rates in this case are presented in [1, 2].

Figure 1 shows the dependences $n_{\rm g}(t)$ for the photogeneration rate $g_0 = 5.75 \times 10^{35}$ m^{-3} s^{-1} (the maximum of the rates presented in Table 1) and the gold ion concentration $N_{\rm t} = 10^{21}$ m^{-3}. One can see that for this relation between g_0 and $N_{\rm t}$, the increase in the nonequilibrium carrier concentration is limited both by Auger recombination and recombination through impurity centres. Simulations showed that, as the photogeneration rate decreases, i.e., upon movement from the centre of the irradiated region to periphery or decreasing pump power, the influence of Auger recombination rapidly weakens and it completely disappears when the photogeneration rate decrease by an order of magnitude.

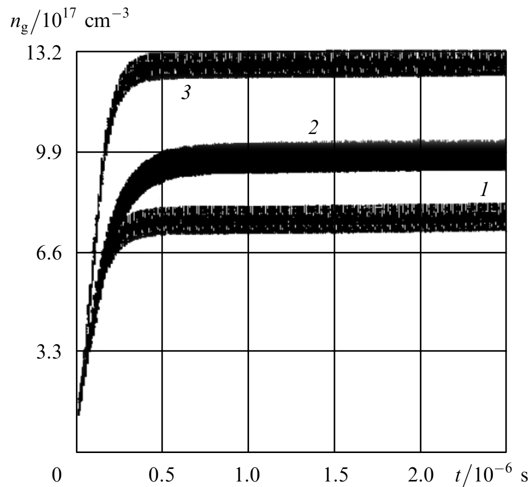

Figure 1. Dynamics of the nonequilibrium carrier concentration in silicon irradiated by a pulsed Ti : sapphire laser upon the simultaneous action of Auger recombination and recombination through impurity centres (*1*), only upon recombination through impurity centres (*2*), and only upon Auger recombination (*3*). The photogeneration rate $g_0 = 5.75 \times 10^{35}$ m^{-3} s^{-1} and the concentration of impurity recombination centres (gold ions) is $N_{\rm t} = 10^{21}$ m^{-3}.

It also follows from the numerical experiment and analytic solution of system (6) that shortly after the beginning of the action of a train of pulses from a Ti : sapphire laser, a periodic variation in the concentration of carriers is established in the part of the Si volume under study, the values of $n_{\rm g}$ and $p_{\rm g}$ being virtually the same. These concentrations exhibit weak, saw-tooth fluctuations with respect to a constant level corresponding to the action of cw radiation, which produces the effective constant photogeneration rate $g_{\rm e}(r,z) = g(r,z)/Q$. Upon variation of $g(r,z)$ within a broad range, i.e., within a greater part of the illuminated Si volume, the modulation depth of the dependence $n_{\rm g}(t)$ did not exceed a few percent. Therefore, electronic processes induced in silicon by radiation from a Ti : sapphire laser and their influence on the RSH generation can be studied theoretically by replacing with good accuracy the real pulsed radiation by cw radiation with the averaged power. In this case, the problem of the distribution of nonequilibrium carriers and a photoinduced electric field becomes stationary: the time derivatives in system (3) and, hence in (6) vanish, and the dependence $g(r,z,t)$ transforms to $g_{\rm e}(r,z)$.

We will assume below that recombination terms have the simplest form [6]

$$R_{\rm n} = \frac{n' - n_0}{\tau_{\rm r}}, \qquad R_{\rm p} = \frac{p' - p_0}{\tau_{\rm r}}, \quad (8)$$

where $\tau_{\rm r}$ is the characteristic recombination time taking into account both Auger recombination and recombination through impurity centres, which we assume identical for electrons and holes.

By solving system (6) in the stationary approximation, we obtain

$$n_{\rm g} = p_{\rm g} = \tau_{\rm r} g_{0\rm e} \exp\left(-\frac{r^2}{R^2} - \alpha z\right) = n_{\rm g0} \exp\left(-\frac{r^2}{R^2} - \alpha z\right), \quad (9)$$

where $n_{\rm g0}$ is the value of the nonequilibrium addition $n_{\rm g}$ at the centre of the illuminated region in the stationary approximation.

4. Calculation of a photoinduced electric field

Due to inequalities (5), we can neglect small additions η and ξ in diffusion-drift terms in system (3) but retain them in recombination terms and the Poisson equation. By using the stability condition substantiated above, we add the first two equations of system (3), express the quantity $\eta - \xi$ from the third equation of the system, and obtain the equation for calculating the spatial distribution of a stationary photoinduced field

$$\frac{1}{r}\frac{\partial}{\partial r}\left\{r\left[E_r\left(\frac{1}{\tau'}\exp\left(-\frac{r^2}{R^2} - \alpha z\right) + \frac{1}{\tau}\right) - \frac{2rU_{\rm d}}{R^2}\frac{1}{\tau'} \times \exp\left(-\frac{r^2}{R^2} - \alpha z\right)\right]\right\} + \frac{\partial}{\partial z}\left[E_z\left(\frac{1}{\tau'}\exp\left(-\frac{r^2}{R^2} - \alpha z\right) + \frac{1}{\tau}\right) - \alpha U_{\rm d}\frac{1}{\tau'}\exp\left(-\frac{r^2}{R^2} - \alpha z\right)\right] = 0, \quad (10)$$

where $1/\tau = 1/\tau_{\rm M} + 1/\tau_{\rm r}$; $\tau_{\rm M} = \varepsilon_0\varepsilon/[(\mu_{\rm n}n_0 + \mu_{\rm p}p_0)e]$ is the characteristic time of the Maxwell relaxation of spontaneous inhomogeneity of the concentration of carriers in an equilibrium electrically neutral semiconductor; $\tau' = \varepsilon_0\varepsilon \times [(\mu_{\rm n} + \mu_{\rm p})n_{\rm g0}e]^{-1}$ is the relaxation time of spontaneous inhomogeneity of the nonequilibrium concentration of carriers at the centre of the illuminated region; and $U_{\rm d} = (D_{\rm n} - D_{\rm p})/(\mu_{\rm n} + \mu_{\rm p})$ is the quantity having the dimensionality of the potential, which is caused by the difference between the diffusion coefficients of electrons and holes and which we call the diffusion stress.

Equation (10) in the Dember effect region should be supplemented with zero boundary conditions $\varphi(r \to \infty, z) = 0$ and $\varphi(r, z \to \infty) = 0$.

The solution of Eqn (10) with the above boundary conditions gives the spatial distributions of the potential and the electric field strength, i.e., it describes the two-dimensional Dember effect in the region under study:

$$\varphi(r,z) = U_{\mathrm{d}} \ln\left[1 + \frac{\tau}{\tau'} \exp\left(-\frac{r^2}{R^2} - \alpha z\right)\right], \quad (11)$$

$$E_r = -\frac{\partial\varphi}{\partial r} = \frac{2rU_{\mathrm{d}}}{R^2}\left[1 + \frac{\tau'}{\tau} \exp\left(\frac{r^2}{R^2} + \alpha z\right)\right]^{-1}, \quad (12)$$

$$E_z = -\frac{\partial\varphi}{\partial z} = \alpha U_{\mathrm{d}}\left[1 + \frac{\tau'}{\tau} \exp\left(\frac{r^2}{R^2} + \alpha z\right)\right]^{-1}. \quad (13)$$

The maximum value of the photoinduced potential in this region

$$\varphi_{\max} = \varphi_{\mathrm{D}} = U_{\mathrm{d}} \ln\left(1 + \frac{\tau}{\tau'}\right) \quad (14)$$

is achieved for $r = z = 0$.

5. Discussion of the results and conclusions

Consider the discussed effect by the example of silicon. Let the wavelength be 690.6 nm. To this wavelength, the maximum effective photogeneration rate of carriers $g_{0\mathrm{e}} = 5.24 \times 10^{30}$ m^{-3} s^{-1} of those presented in Table 1 corresponds. The characteristic recombination time through impurity centres in Si is 10^{-6} s, and for the indicated value of $g_{0\mathrm{e}}$ in the central part of the irradiated region, Auger recombination will dominate. By using the recombination term (7) in (6), we obtain that the carrier concentration at the centre of the irradiated region is $n_{\mathrm{g}0} = (g_{0\mathrm{e}}/8a_{\mathrm{A}})^{1/3} = 1.18 \times 10^{24}$ m^{-3}. Let the equilibrium concentrations of carriers be $n_0 = 1.45 \times 10^{21}$ m^{-3} and $p_0 = 1.45 \times 10^{11}$ m^{-3}, which corresponds to nondegenerate n-Si with the specific resistance 3.5 Ω cm.

The values of the parameters $\mu_{\mathrm{n,p}}$ and $D_{\mathrm{n,p}}$ depend on the carrier concentration and can substantially differ from their equilibrium values in the irradiation regime under study. We calculated mobilities $\mu_{\mathrm{n,p}}$ for the specified value of $n_{\mathrm{g}0}$ by using expressions from [8], while the corresponding diffusion coefficients $D_{\mathrm{n,p}}$ were calculated from the generalised Einstein formulas [6]. Our calculations gave the following values: $\mu_{\mathrm{n}} = 0.0230$ m^2 V^{-1} s^{-1}, $\mu_{\mathrm{p}} = 0.0108$ m^2 V^{-1} s^{-1}, $D_{\mathrm{n}} = 40 \times 10^{-5}$ m^2 s^{-1}, and $D_{\mathrm{p}} = 17 \times 10^{-5}$ m^2 s^{-1}. In this case, $\tau \approx \tau_{\mathrm{M}} = 2.39 \times 10^{-11}$ s, $\tau' = 2.0 \times 10^{-14}$ s, and $U_{\mathrm{d}} = 6.8$ mV.

By using these parameters, we calculated from (11)–(13) the spatial distributions of the potential and strength of the photostimulated field in the Dember effect region (Figs 2–4).

Our calculation showed that the photostimulated potential in the axial region of the beam was a few tens of millivolts. Its maximum value φ_{D} is achieved at the boundary of the near-surface plane SCR and in the Dember effect region and is calculated from expression (14). For a given example, $\varphi_{\mathrm{D}} = 48$ mV.

As shown in papers [9, 10], the RSH intensity for centrally symmetric semiconductors strongly depends on the electric field strength in a thin near-surface SCR, which is determined by the potential difference applied to it. Because the potential inside a semiconductor was assumed zero in previous papers (see, for example, [4, 9–11]), the potential difference was assumed equal to the surface potential φ_{sc}, which was produced either by a surface charge or was externally applied [9]. Note that the value of $|\varphi_{\mathrm{sc}}|$ was

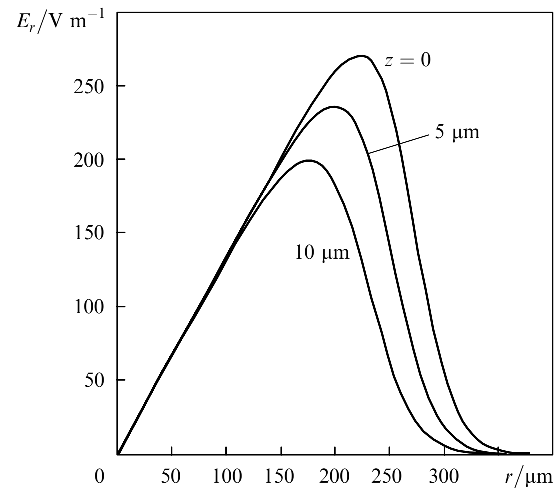

Figure 2. Dependences of the radial component E_r of the photoinduced electric field strength on the radial coordinate r for different values of the longitudinal coordinate z.

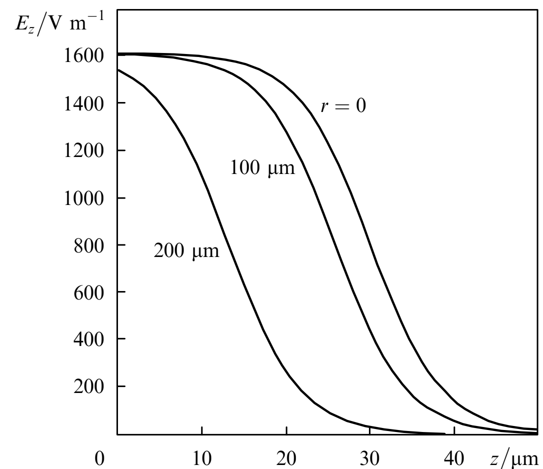

Figure 3. Dependences of the axial component E_z of the photoinduced electric field strength on the longitudinal coordinate z for different values of the radial coordinate r.

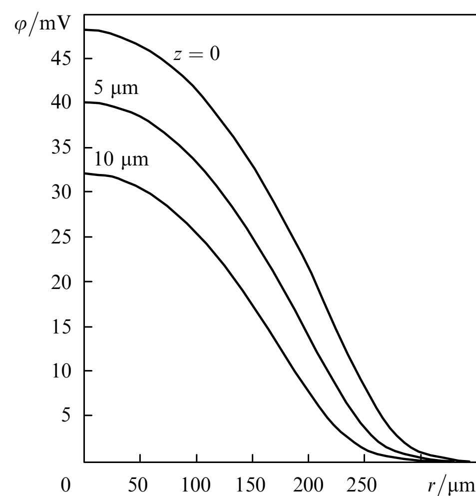

Figure 4. Dependences of the potential φ of the photoinduced electric field on the radial coordinate r for different values of the longitudinal coordinate z.

varied within a few tens of millivolts, which is comparable with the values of φ_D found earlier. Therefore, the mechanism of influence of photostimulated electronic processes on the nonlinear optical response of the silicon surface described in papers [1, 2] and caused by the SCR transformation also takes place when a Ti : sapphire laser is used. To take this influence into account, it is necessary to introduce some corrections to the generation theory, which in the first approximation account for the narrowing of the near-surface SCR and involve the replacement of φ_{sc} by $\varphi_{sc} - \varphi_D$.

The characteristic thickness of the nonequilibrium plane near-surface SCR, i.e., the Debye screening lens L_{Db} changes from 2.7 to 3.4 nm when the photogeneration rate is varied in the range shown in Table 1. In this case, the relation $4\pi L_{Db}/\lambda \ll 1$ is fulfilled, and the RSH parameters can be calculated using the theory developed in [10].

Note that, when a Ti : sapphire laser is used, the photoinduced potential of the volume can be assumed constant, whereas in the case of a Nd : YAG laser this potential substantially changes during each pulse.

The characteristic depth of the Dember effect region is determined by the characteristic penetration depth d of the pump and lies between 4230 and 12 760 nm in the wavelength range under study. The characteristic depth of a layer generating the RSH varies from ~ 10 to ~ 120 nm, i.e., this layer overlaps with the Dember effect region, but the thickness of the overlap region is rather small compared to d. In addition, as shown above, the Dember field strength does not exceed 2×10^3 V m^{-1}, which is much lower than the strength of the electric field producing nonlinear optical effects. Therefore, the contribution of the overlap region can be neglected.

The concentration of nonequilibrium carriers found above is considerably lower than that of valence electrons, which is 2×10^{29} m^{-3} for silicon. Therefore, the influence of photogeneration of nonequilibrium carriers on the nonlinear susceptibilities of silicon can be neglected.

References

1. Baranova I.M., Evtyukhov K.N., Muravyev A.N. *Proc. SPIE Soc. Opt. Eng.*, **4749**, 183 (2002).
2. Baranova I.M., Evtyukhov K.N., Murav'ev A.N. *Kvantovaya Elektron.*, **33**, 171 (2003) [*Quantum Electron.*, **33**, 171 (2003)].
3. Dadap J.I., Xu Z., Hu X.F., Downer M.C., Russel N.M., Ekerdt J.G., Aktsipetrov O.A. *Phys. Rev. B*, **56** (20), 13367 (1997).
4. Aktsipetrov O.A., Fedyanin A.A., Melnikov A.V., Mishina E.D., Rubtsov A.N., Anderson M.H., Wilson P.T., ter Beek M., Hu X.F., Dadap J.I., Downer M.C. *Phys. Rev. B*, **60** (12), 8924 (1999).
5. Aspnes D.E., Studna A.A. *Phys. Rev. B*, **27** (2), 985 (1983).
6. Bonch-Bruevich V.L., Kalashnikov S.G. *Fizika poluprovodnikov* (Physics of Semiconductors) (Moscow: Nauka, 1977).
7. Akhmanov S.A., Emel'yanov V.I., Koroteev N.I., Seminogov V.I. *Usp. Fiz. Nauk*, **144**, 675 (1985).
8. Novikov V.V. *Teoreticheskie osnovy mikroelektroniki* (Theoretical Foundations of Microelectronics) (Moscow: Vysshaya Shkola, 1972).
9. Lüpke G. *Surface Sci. Rep.*, **35**, 75 (1999).
10. Baranova I.M., Evtyukhov K.N. *Kvantovaya Elektron.*, **24**, 347 (1997) [*Quantum Electron.*, **27**, 336 (1997)].
11. Aktsipetrov O.A., Baranova I.M., Evtyukhov K.N., et al. *Kvantovaya Elektron.*, **19**, 869 (1992) [*Quantum Electron.*, **22**, 807 (1992)].